Structural Correlations and Vinyl Influences in Resonance Raman Spectra of Protoheme Complexes and Proteins

S. Choi,[†] T. G. Spiro,*[,†] K. C. Langry,[‡] K. M. Smith,[‡] D. L. Budd,[‡] and G. N. La Mar[‡]

Contribution from the Departments of Chemistry, Princeton University, Princeton, New Jersey 08544, and the University of California, Davis, California 95616.
Received June 19, 1981

Abstract: Resonance Raman spectra obtained with B (Soret) and Q_1 (β) band excitations are compared for protoheme complexes displaying several oxidation, spin, and ligation states: $Im_2Fe^{III}PP^+$ (Im = imidazole, PP = protoporphyrin IX), $Im_2Fe^{II}PP$, $ClFe^{III}PP$, $(Me_2SO)_2Fe^{III}PP^+$ (Me_2SO = dimethyl sulfoxide), and (2-MeIm)$Fe^{II}PP$ (2-MeIm = 2-methylimidazole). The effects of C_α and C_β vinyl deuteration reveal the same extensive pattern of vinyl modes as seen in NiPP (see preceding paper). Vinyl influences on the porphyrin skeletal frequencies appear to include both kinematic and conjugative effects. Previously observed correlations with porphyrin core size have been augmented; *all* the skeletal modes above 1450 cm^{-1} show a negative linear dependence on C_t–N (center-to-nitrogen distance), with slopes that depend on the extent of methine bridge bond involvement in the modes. The complex $Im_2Fe^{II}PP$ shows large deviations from these correlations, associated with d_π back-bonding. The deviations depend on the vibrational mode symmetries in a manner plausibly related to the nodal pattern of the porphyrin e_g^* acceptor orbitals. Comparison of the complexes with deoxyMb (Mb = myoglobin), $Mb^{III}F$, and $Hb^{III}F$ (Hb = hemoglobin) shows protein influences to be small for modes above 1300 cm^{-1} but substantial for modes in the 900–1300-cm^{-1} region, which have appreciable contributions from pyrrole-substituent stretching. In particular deoxyMb and $Mb^{III}F$, but not $Hb^{III}F$, show a new band at ~1120 cm^{-1}, which shifts up on C_α deuteration and is assignable to pyrrole–vinyl stretching. This band correlates with an IR band of NiPP at 1118 cm^{-1}; it is evidently activated by a specific symmetry-lowering effect of Mb, which is suggested to be an electrostatic field near the vinyl groups.

While metalloporphyrin resonance Raman (RR) spectra have been studied in considerable detail and a number of regularities have been noted,[1] a deeper understanding is needed to bring RR spectroscopy to its full potential as a probe of heme protein structure. A systematic analysis has been made possible by the complete assignment of the in-plane vibrational modes of NiOEP (OEP = octaethylporphyrin) by Kitagawa et al.[2] and by the elucidation of vinyl influences on the NiPP (PP = protoporphyrin IX) spectra in the preceding paper.[3] In the present work we reexamine the RR spectra of a series of Fe–PP complexes and their vinyl C_α and C_β deuterated forms, with 4131-, 4579-, 4880-, and 5145-Å excitation, near resonance with the B and Q_1 absorption bands. The vinyl influences are found to be similar to those observed for NiPP, modified by the metal-associated shifts in the porphyrin skeletal modes. The cataloguing of the skeletal modes has revealed an extensive pattern of structure-dependent frequencies. Whereas a negative linear dependence on porphyrin core size has previously been demonstrated for three identifiable skeletal modes,[4-6] the present analysis shows that this correlation exists for all the skeletal modes above 1450 cm^{-1}, the slopes varying with the normal mode composition. The complex $Im_2Fe^{II}PP$ (Im = imidazole) deviates from these correlations in a manner plausibly related to Fe^{II}–porphyrin π back-bonding.[6-9] Only the ~1370 cm^{-1} "oxidation-state marker" band[7,10] shows a clear-cut dependence on oxidation state per se, presumably due to polarization of the pyrrole C_a–N bonds.

RR spectra of myoglobin (Mb) derivatives showed the effect of the protein to be slight for the higher frequency skeletal modes, except that metMb fluoride and deoxyMb showed activation of an IR mode at ~1120 cm^{-1} assignable to ring–vinyl stretching. This activation is not seen in hemoglobin.

This study is limited to the RR bands above 1000 cm^{-1}. The region below 1000 cm^{-1} is taken up in a subsequent paper,[11] in which evidence for out-of-plane porphyrin mode enhancement is presented.

Experimental Section

All iron–protoporphyrin complexes were prepared from hemin chloride (Sigma), or its C_α or C_β vinyl deuterated forms, whose preparation is described elsewhere.[12] It was dissolved in a minimum amount of 0.1 M NaOH and diluted with H_2O to a concentration of 0.5 mM (pH ~10.5). Excess imidazole, purified by sublimation and/or recrystallization in toluene (to remove fluorescent impurities), was added to produce $Im_2Fe^{III}PP^+$. A slight excess of solid sodium dithionite (BDH) was then added to produce $Im_2Fe^{II}PP$. (2-MeIm)$Fe^{II}PP$ was produced by the same procedure, replacing imidazole with 2-methylimidazole (purified by sublimation). $(Me_2SO)_2Fe^{III}PP^+$ was prepared by dissolving hemin chloride in dimethyl-d_6 sulfoxide (the deuteration removes interfering solvent Raman bands from the region of interest); its absorption spectrum matched that of purified $[(Me_2SO)_2Fe^{III}PP]ClO_4$.[6] mesoPorphyrin complexes were prepared in the same way, starting with mesohemin chloride made by the standard method[13] of Fe insertion into mesoporphyrin IX dimethyl ester (Man-Win Chem.) and hydrolysis. $[Fe^{III}OEP]Cl$ was made by insertion of Fe into octaethylporphyrin.[13] Excess imidazole was added to $[Fe^{III}OEP]Cl$ in CH_2Cl_2 for $Im_2Fe^{III}OEP$.

Sperm whale myoglobin (Miles) was purified by Sephadex chromatography (G-25) and isoelectric focusing (G-100 superfine gel with Ampholine pH 6–8). Myoglobin was reconstituted with hemin-d_α and -$d_2\beta$ chloride by standard methods.[14] Methemoglobin was prepared by oxidation of oxyhemoglobin with excess potassium ferricyanide followed by Sephadex G-25 chromatography with 0.05 M phosphate buffer (pH 6.6). Metmyoglobin and methemoglobin fluoride samples were prepared by

[†] Princeton University.
[‡] University of California, Davis.

(1) For recent reviews, see: (a) Spiro, T. G. *Isr. J. Chem.* **1981**, *21*, 81. (b) Asher, S. A. (1981) "Methods in Enzymology, Hemoglobin Part", Antonini, E., Bernardi, L. R., Chiancone, E., Eds.; Academic Press: New York, in press. (c) Felton, R. H.; Yu, Nai-Teng. In "The Porphyrins"; Dolphin, D., Ed.; Academic Press: New York, 1978; Vol. III, Part A, pp 347–388. (d) Kitagawa, T.; Ozaki, Y.; Kyogoku, Y. *Adv. Biophys.* **1978**, *11*, 153.
(2) (a) Kitagawa, T.; Abe, M.; Ogoshi, H. *J. Chem. Phys.* **1978**, *69*, 4516. (b) Abe, M.; Kitagawa, T.; Kyogoku, Y. *Ibid.* **1978**, *69*, 4526.
(3) Choi, S.; Spiro, T. G.; Langry, K. C.; Smith, K. M. *J. Am. Chem. Soc.*, preceding paper in this issue.
(4) Spaulding, L. D.; Chang, C. C.; Yu, N. T.; Felton, R. H. *J. Am. Chem. Soc.* **1975**, *97*, 2517.
(5) Huong, P. V.; Pommier, J.-C. *C. R. Hebd. Seances Acad. Sci., Ser. C* **1977**, *285*, 519.
(6) Spiro, T. G.; Stong, J. D.; Stein, P. *J. Am. Chem. Soc.* **1979**, *101*, 2648.
(7) Spiro, T. G.; Strekas, T. *J. Am. Chem. Soc.*, **1974**, *96*, 338.
(8) Kitagawa, T.; Iizuka, T.; Saito, M.; Kyogoku, Y. *Chem. Lett.* **1975**, 849.
(9) Spiro, T. G.; Burke, J. M. *J. Am. Chem. Soc.* **1976**, *98*, 5482.
(10) Rimai, L.; Salmeen, I.; Petering, D. H. *Biochemistry* **1975**, *14*, 378.
(11) Choi, S.; Spiro, T. G., submitted for publication.
(12) Budd, D. L.; La Mar, G. N.; Langry, K. C.; Smith, K. M.; Nayyir-Mazhir, R. *J. Am. Chem. Soc.* **1979**, *101*, 6091.
(13) Buchler, J. W. In "Porphyrins and Metalloporphyrins"; Smith, K. M., Ed., American Elsevier: New York, 1976; pp 157–231.
(14) Teale, F. W. J. *Biochim. Biophys. Acta* **1959**, *35*, 543.

0002-7863/82/1504-4345$01.25/0

Table I. RR Frequencies (cm^{-1}) for PP Complexes, with Observed Shifts on C_α and/or C_β Vinyl Deuteration, and the Frequency Differences for Corresponding OEP and/or MP Complexes

mode[a,b]			Ni		Im_2Fe^{III}			Im_2Fe^{II}		$ClFe^{III}$	$(Me_2SO)_2Fe^{III}$		(2-MeIm)Fe^{II}	
			PP	ΔOEP[c]	PP	ΔMP[c]	ΔOEP	PP	ΔMP	PP	PP	ΔMP	PP	ΔMP
ν_{10}	B_{1g}	C_aC_m	1655		1640			1617		1626	1610		1604	
ν(C=C)			1634		1620			1620		1626	1621		1622	
ν_{37}	E_u	C_bC_b	1610		1602			1604		1591	1580		1583	
ν_{19}	A_{2g}	C_aC_m	1603		1586			1583		1571	1560		1550	
ν_2	A_{1g}	C_bC_b	1593	+9	1579	+13	+12	1584	+15	1570	1559	+20	1562	+19
ν_{11}	B_{1g}	C_bC_b	1575		1562	+9	+7	1539	+6	1553	1545		1547	+7
ν_{38}	E_u	C_aC_m	1566		1554			1560		1533	1518		1521	
ν_3	A_{1g}	C_aC_m	1519		1502			1493		1491	1480		1471	
ν_{28}	B_{2g}	C_aC_m	1482		1469			1461		1453	1447			
δ_S(=CH_2) (1)			1434		1435			1431		1435	1429		1426	
ν_{29}	B_{2g}	C_aC_b	1401	+8	1402	+5	+5	1390	4	1403	1392		1392	+8
ν_{20}	A_{2g}	C_aN	1399	3	1399		4	1392	+2	1403	1389		1401	
ν_4	A_{1g}	C_aN	1381	+2	1373		+6	1359		1373	1370		1357	
δ_S(=CH_2) (2)			1343		1346			1337		1340			1338	
ν_{21}	A_{2g}	$\delta(C_mH)$	1305		1306			1305		1309	1313		1302	
		δ(CH=)	1305		1306			1305		1308	1311		1305	
$\nu_5 + \nu_9$	A_{1g}		1254	+7	1260			1254	9	1260	1239		1285	26
ν_{13}	B_{1g}	$\delta(C_mH)$	1234	14	1230		5	1225	+3	1228	1225	+2	1227	6
$\nu_5 + \nu_{18}$	B_{1g}			(1220)[d]										
$\nu(C_b-C_\alpha)$ (1) (ν_{30}, β_{29})			1167	8	1167	7	8	1174	(1154)	1170	1170		1170	9
$\nu_6 + \nu_8$	A_{1g}		1130	+8	1130		+11	1130		1130	1130	+3	1130	6
ν_{22}	A_{2g}	C_aN	1125	+4	1125			1125		1127			1122	
δ_{as}(=CH_2)			1089		1089			1089		1089			1087	
ν_5	A_{1g}	C_bS		(1025)			(1029)		(1020)					
ν_{45}	E_u	C_aN	999		997	+4		995	+1				999	10
γ(CH=)			999		1008			1008		1008			1005	

[a] Mode numbers and skeletal assignments follow Kitagawa et al.[2] and ref 3. [b] Observed vinyl deuteration downshifts or upshifts (+) (cm^{-1}) are listed here in the order: NiPP-d_α, NiPP-$d_{2\beta}$; $[Im_2Fe^{III}PP]^+$-d_α, $[Im_2Fe^{III}PP]^+$-$d_{2\beta}$; $Im_2Fe^{II}PP$-d_α; $ClFe^{III}PP$-d_α; $[(Me_2SO)_2Fe^{III}PP]^+$-d_α; (2-MeIm)Fe^{II}PP-d_α: ν(C=C) 24, 34; 18, –; 16; 15; 9; 18. ν_2 3, –; 3, –; 4; 4; –; –. δ_S(=CH_2) (1) 9, –; 10, –; 12; 10; 5; 10. ν_{29} –, +8; –, –; –; –; –. ν_S(=CH_2) (2) 5, –; 3; –; 2; –; –; –. δ(CH=) 209, 0; 210, 0; 210; –; –; 209. $\nu(C_b-C_\alpha)$ (1) +15, 0; +10, 0; +13; +13; +15; +13. δ_{as}(=CH_2) 51, –; –; –; –; –; –; –. γ(CH=) –; –; –; –; –; –; –; –. (– means the band was unobserved or the shift undetermined due to overlaps). [c] Frequency downshifts observed on substituting OEP (ΔOEP) or MP (ΔMP) for PP; upshifts are indicated by +. [d] ( ) Bands seen in OEP or MP complexes, which are not observed for PP.

addition of purified protein to phosphate buffer solution (0.05 M, pH 6.5) containing KF (0.1 M). Deoxymyoglobin was prepared by addition of dithionite anaerobically to the metmyoglobin solution equilibrated with Ar gas.

RR spectra were obtained as described elsewhere.[3,6]

Results and Discussion

Assignments. RR spectra were recorded for $[Im_2Fe^{III}PP]Cl$ as the free dipropionate in water (pH 10.5) and the dimethyl ester in CH_2Cl_2. Although a split B (Soret) absorption band (λ_{max} = 406 and 432 nm) gives evidence of aggregation is aqueous solution,[15] only two frequency differences were observed between CH_2Cl_2 and H_2O solutions: the 1375-cm^{-1} p (polarized) band (oxidation state marker) shifted down slightly to 1373 cm^{-1} and the 1315-cm^{-1} ap (anomalously polarized) band shifted to 1310 cm^{-1}. In all other respects, the spectra were unaffected by esterification or change of solvent.

Figure 1 shows 4579-Å excitation spectra of $Im_2Fe^{III}PP^+$ and for the C_α vinyl deuterated form. The spectrum of the C_β deuterated form (not shown) was also obtained. The deuteration shifts reveal the same pattern of vinyl modes as for NiPP.[3] The C=C stretch is found at 1620 cm^{-1}, 14 cm^{-1} lower than in NiPP; it shifts down on C_α or C_β deuteration and couples with the porphyrin skeletal mode (ν_2, A_{1g}) at 1579 cm^{-1}, as shown by the 3-cm^{-1} C_α deuteration shift of the latter. Two =CH_2 scissors modes, coupled respectively to ν_{29} (B_{2g}) and ν_{20} (A_{2g}), are found at 1435 and 1346 cm^{-1}, essentially the same frequencies as for NiPP; they shift down slightly on C_α deuteration and disappear on C_β deuteration. The CH= wag appears at 1306 cm^{-1}, as in NiPP, shifting down to 1096 cm^{-1} upon C_α deuteration. The C_b–vinyl stretch appears at 1167 cm^{-1}. As in the case of NiPP, C_α deuteration shifts this band up by 10 cm^{-1} and induces RR activity for a mode at 1154 cm^{-1}, identified as a B_{2g} mode (ν_{30}) of NiOEP. Finally the CH= out-of-plane deformation is found at 1008 cm^{-1}, 9 cm^{-1} higher than for NiPP; it is a distinct shoulder on the 997-cm^{-1} skeletal mode (ν_{45}, E_u) and disappears on C_α deuteration.

The skeletal mode assignments follow those of Kitagawa et al.,[2] as modified in the preceding paper.[3] Table I lists the RR frequencies for all the PP complexes included in this study, as well as observed shifts on C_α and C_β vinyl deuteration, and also the frequency differences for corresponding OEP and/or MP (MP = mesoporphyrin IX) complexes. Correlations among the spectra were made on the basis of band polarizations and enhancement patterns.

Structure Correlations. (a) Core Size. Figures 2 and 3 compare spectra of NiPP, as the dimethyl ester in CCl_4, with those of $Im_2Fe^{III}PP^+$, $Im_2Fe^{II}PP$, $ClFe^{III}PP$, (2-MeIm)Fe^{II}PP, and $(Me_2SO)_2Fe^{III}PP^+$, as the free propionates in H_2O, or in Me_2SO for the last complex. These complexes were chosen as representative of different oxidation, spin, and coordination numbers encountered in heme proteins. X-ray structural data[16-22] are available for all of them, although not necessarily on the protoporphyrin complex itself; however, variation in peripheral sub-

(15) Gallager, W. A.; Elliot, W. B. *Ann. N.Y. Acad. Sci.* **1973**, *206*, 463.

(16) Hoard, J. L. In "Porphyrins and Metalloporphyrins"; Smith, K. M., Ed.; American Elsevier: New York, 1975; pp 317–376.

(17) Cullen, D. L.; Meyer, E. F., Jr. *J. Am. Chem. Soc.* **1974**, *96*, 2095.

(18) Collins, D. M.; Countryman, R.; Hoard, J. L. *J. Am. Chem. Soc.* **1972**, *94*, 2066.

(19) Radonovich, L. J.; Bloom, A.; Hoard, J. L. *J. Am. Chem. Soc.* **1972**, *94*, 2073.

(20) (a) Hoard, J. L. *Science (Washington, D.C.)* **1971**, *174*, 295. (b) Hoffman, A. B.; Collins, D. M.; Day, V. W.; Fleischer, E. B.; Srivastava, T. S.; Hoard, J. L. *J. Am. Chem. Soc.* **1972**, *94*, 3620. (c) Hoard, J. L.; Hamor, M. J.; Hamor, T. A.; Caughy, W. S. *Ibid.* **1965**, *87*, 2312. (d) Koenig, D. F. *Acta Crystallogr.* **1965**, *18*, 663.

(21) Hoard, J. L., Scheidt, W. R. *Proc. Natl. Acad. Sci. U.S.A.* **1973**, *70*, 3919; **1974**, *70*, 1578.

(22) Mashiko, T.; Kastberm, M. E.; Spartalian, K.; Scheit, R. W.; Reed, C. A. *J. Am. Chem. Soc.* **1978**, *100*, 6354.

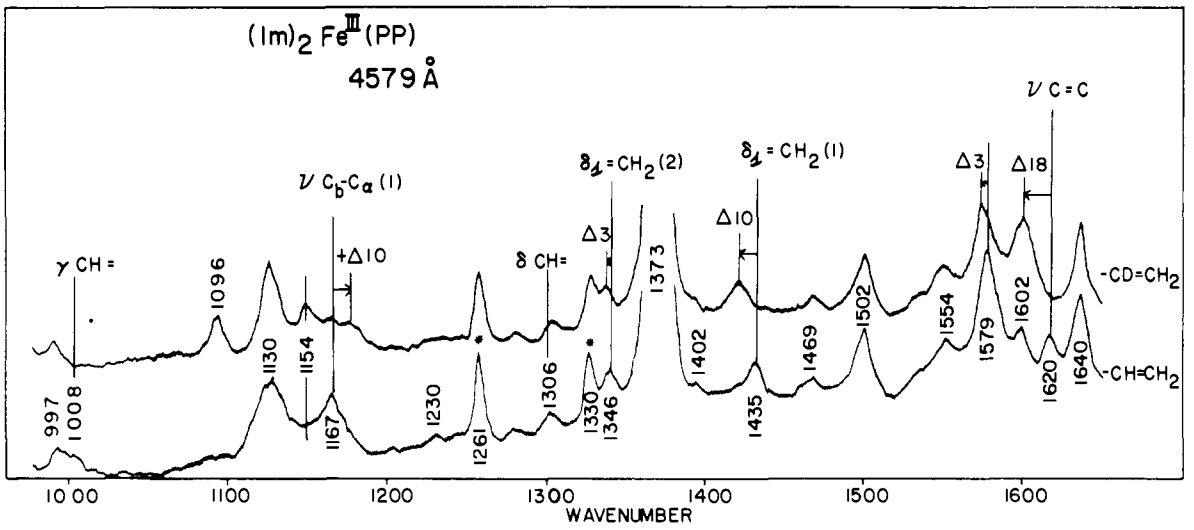

Figure 1. Raman spectra of $Im_2Fe^{III}PP^+$ and $Im_2Fe^{III}PP^+$-d_α in H_2O (~0.5 mM, pH 10.5), excited with the 4579-Å Ar^+ laser line (100 mW); slit width, 5 cm^{-1}. Bands marked with * are due to excess imidazole.

stitution is known to have no appreciable effect on the skeletal geometry.[16] The spectra were obtained with 4131-, 4579-, 4880-, and 5145-Å excitation to bring out different bands. Although the absorption spectra vary, these excitation wavelengths are close to the absorption band maxima of the B (Soret) and Q_1 (β) transitions. Variable excitation is especially important in sorting out RR frequencies in crowded regions of the spectrum, e.g., the 1500–1600-cm^{-1} region. Thus ν_2 (A_{1g}) and ν_{19} (A_{2g}) are nearly coincident, but the former appears in B excitation, whereas the latter, which is identified via its anomalous polarization, is enhanced with Q_1 excitation. Likewise ν_{38} (E_u) appears only in B excitation, while the nearby ν_{11} (B_{1g}) is stronger with Q_1 excitation. Usually ν_{11} is higher than ν_{38}, but for $Im_2Fe^{II}PP$ the order is reversed. Table I correlates the various modes for these complexes. (In several cases the vinyl mode assignments were checked with the d_α derivatives.)

As is apparent from the figures and also from Table I, there is a general lowering of the band frequencies above 1450 cm^{-1}, except for ν(C=C), along the series of complexes. This trend is readily correlated with the size of the porphyrin core, as demonstrated in Figure 4, where the frequencies are plotted against C_t–N, the porphyrin center-to-pyrrole nitrogen distance. A correlation with core size was first noted by Spaulding et al.[4] for the ap band near 1580 cm^{-1} (ν_{19}, or band IV[9]). The linearity of the correlation was later established for this band and two others,[5,6] ν_{10} (band V[9]) and ν_3 (band II[9]), all of which had earlier been identified[7] as being sensitive to the spin state. Recently Callahan and Babcock[23] have noted a similar, but weaker, correlation for ν_2.

The present results establish a core-size influence for all the skeletal modes above 1450 cm^{-1}; the vinyl ν(C=C), at ~1620 cm^{-1} is affected very little, however. It had been argued[6] that porphyrin core expansion lowered the C_a–C_m stretching frequencies by specifically weakening the methine bridge bonds. While core-size sensitivity is now seen to be universal among the high-frequency skeletal modes, support for a dominant methine bridge influence can still be found in the slopes of the correlations, given in Table II. The higher slopes belong to modes with dominant C_a–C_m stretching contributions, according to the calculations of Abe et al.,[2b] ν_{10} (B_{1g}), ν_{19} (A_{2g}), and ν_3 (A_{1g}). The lower slopes belong to modes with dominant C_b–C_b stretching contributions, ν_2 (A_{1g}) and ν_{11} (B_{1g}). The two E_u modes seem to be out of order, since ν_{37} and ν_{38} are calculated to be mainly C_a–C_m and C_b–C_b, respectively, but the former has a low slope and the latter a higher one. The meso-deuteration shifts of these two modes (greater for ν_{38}) are not reproduced by the calculation,[2b] however, and we suspect that the normal mode compositions are in error.

(23) Callahan, P. M.; Babcock, G. T. *Biochemistry* **1981**, *20*, 952.

Table II. Porphyrin Core-Size Correlation Parameters for High-Frequency Skeletal Modes

mode	PED[a]	K,[b] cm^{-1}/Å	A,[b] Å	ΔIm_2Fe^{II}, cm^{-1} [c]
ν_{10} (B_{1g})	C_aC_m (49)	517.2	5.16	−17
ν_{38} (E_u)	C_bC_b (53)[d]	551.7	4.80	+19
ν_{19} (A_{2g})	C_aC_m (67)	494.3	5.20	+3
ν_3 (A_{1g})	C_aC_m (41)	448.3	5.35	−5
ν_{28} (B_{2g})	C_aC_m (52)	402.3	5.64	−3
ν_2 (A_{1g})	C_bC_b (60)	390.8	6.03	+9
ν_{37} (E_u)	C_aC_m (36)[d]	356.3	6.48	+10
ν_{11} (B_{1g})	C_bC_b (57)	344.8	6.53	−21

[a] Percentage contribution of the major contributor (C_a–C_m or C_b–C_b stretching) to the potential energy distribution, according to Abe et al.[2b] [b] Slope and intercept for the relation $\bar{\nu} = K(A - d)$; $\bar{\nu}$ = mode wavenumber and d = porphyrin center-to-pyrrole nitrogen distance, C_t–N. [c] Deviations for $Im_2Fe^{II}PP$ from the frequencies expected on the basis of its core size. [d] The calculated ν_{37} and ν_{38} mode compositions are believed to be in error; see text.

(b) π Back-Bonding. One of the complexes, $Im_2Fe^{II}PP$, deviates systematically from the correlations. These deviations are listed in Table II. The points fall well below the lines for the high-frequency B_{1g} (ν_{10} and ν_{11}) modes but well above the lines for the E_u (ν_{37} and ν_{38}) modes. The B_{1g} modes (bands V and III[9]) have previously been identified as being sensitive to the Fe oxidation state or the extent or π back-bonding. When Im is replaced in $Im_2Fe^{II}PP$ with ligands that are effective π acceptors,[9] the frequencies of these bands shift to higher frequencies, approaching those of $Im_2Fe^{III}PP^+$, in which a d_π electron has been completely removed. The lowering of these frequencies in $Im_2Fe^{II}PP$ is attributable to the decrease in ring π bonding associated with d_π donation into the porphyrin π^* orbitals (e_g). Of the complexes included in this study, $Im_2Fe^{II}PP$ is the only one for which d_π donation is expected to be effective. Oxidation to Fe^{III} lowers the d_π energy, while conversion to the high-spin (2-MeIm)$Fe^{II}PP$ decreases the π^*–d_π overlap due to the lengthened Fe–pyrrole bonds and the out-of-plane displacement of the Fe. The deviations of $Im_2Fe^{II}PP$ from the correlations can be understood on this basis.

However, the fact that negative deviations are observed for the B_{1g} modes, but positive ones for the E_u modes, adds an interesting new element. This symmetry-specific effect must be related to the nodal patterns of the e_g (π^*) orbitals, a diagram[24] of which is given in Figure 5. It can be seen that the atomic orbital phasing is antibonding for one pair of opposite pyrrole C_b–C_b bonds but bonding for the other pair. Thus population of this orbital favors

(24) Longuet-Higgins, H. C.; Rector, C. W.; Platt, J. R. *J. Chem. Phys.* **1950**, *18*, 1174.

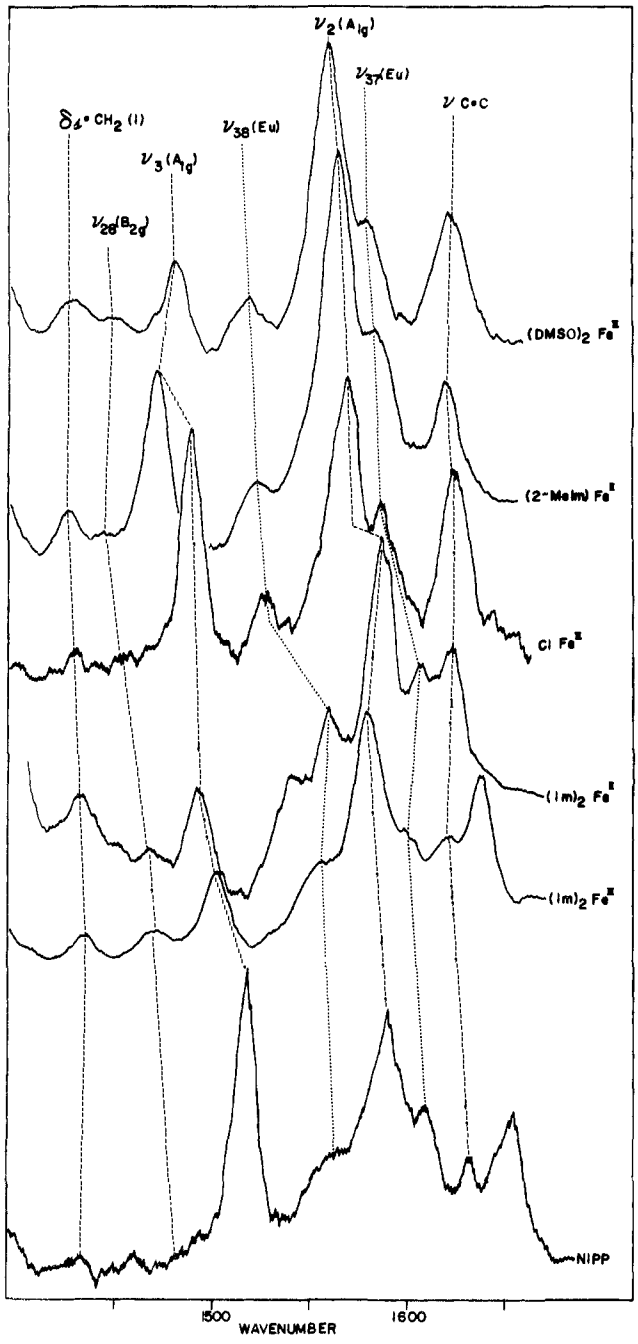

Figure 2. Raman spectra with B (Soret) band excitation for several PP complexes: $(Me_2SO)_2Fe^{III}PP^+$ in Me_2SO; (2-MeIm)Fe^{II}PP, $ClFe^{III}$PP, $Im_2Fe^{II}PP$, $Im_2Fe^{III}PP^+$, all in water (pH 10.5); NiPP (as the dimethyl ester), in CCl_4. Concentrations are ~0.5 mM. λ_0 = 4131 Å for $(Me_2SO)_2Fe^{III}PP^+$, $ClFe^{III}$PP, and NiPP; λ_0 = 4579 Å for (2-MeIm)-Fe^{II}PP, $Im_2Fe^{II}PP$, and $Im_2Fe^{III}PP^+$; slit width, 5 cm^{-1}.

stretching of one pair of opposite pyrrole bonds and simultaneous contraction of the other pair. This motion has $\mathbf{B}_{1g}$ symmetry, and the B_{1g} ring modes can therefore be expected to show specific decreases in their force constants and frequencies. In the E_u modes, however, stretching of adjacent bonds is accompanied by contraction of opposite ones. This phasing cancels the effects of e_g orbital occupancy and may explain the elevation of the E_u frequencies. Interestingly, the A_{1g} modes show both kinds of deviations, although they are smaller in extent than those of the B_{1g} and E_u modes. The $Im_2Fe^{II}PP$ points fall above the line for ν_2 but below the line for ν_3. In the A_{1g} modes, all bonds of a given type are expanded, or contracted, together. This phasing neither reinforces nor suppresses the e_g nodal pattern. Finally the points do not deviate from the lines for the A_{2g} (ν_{19}) and B_{2g} (ν_{28}) lines. Because these modes are antisymmetric with respect to the mirror

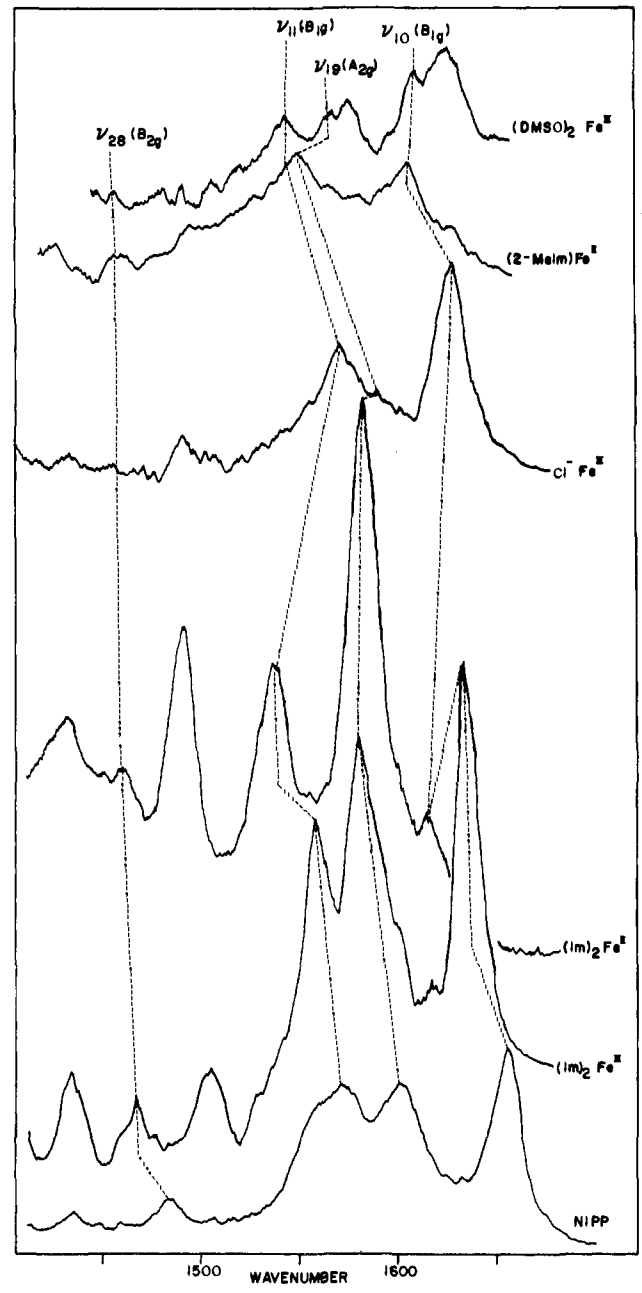

Figure 3. Raman spectra with Q_1 (β) band excitation, for PP complexes, as in Figure 2. λ_0 = 4880 Å for $(Me_2SO)_2Fe^{III}PP^+$ and $ClFe^{III}$PP; λ_0 = 5308 Å for (2-MeIm)Fe^{II}PP; λ_0 = 5145 Å for $Im_2Fe^{II}PP$, $Im_2Fe^{III}PP^+$, and NiPP; slit width, 10 cm^{-1}.

planes that bisect the pyrrole rings, they have no contribution from C_b–C_b stretching.

(c) Doming. It should be noted that the slopes and intercepts of the present linear correlations differ somewhat from those previously determined[5,6] for bands II, IV, and V on the basis of data for a wide range of metalloporphyrins. Several iron derivatives were observed to deviate from the wider correlations, and these deviations were attributed largely to pyrrole ring tilting in domed or ruffled porphyrin structures.[6] Another possibility, however, is that the C_t–N dependence is itself somewhat dependent of the nature of the metal ions. The present correlations are anchored by NiPP and $(Me_2SO)_2Fe^{III}PP^+$. The intermediate points for $Im_2Fe^{III}PP^+$ (slightly ruffled[16]) and $ClFe^{III}$PP (Fe out-of-plane and very slightly domed[16]) fall very near the lines for all modes.

The effect of ring tilting is probably seen most clearly in comparing the data points for (2-MeIm)Fe^{II}PP and $(Me_2SO)_2Fe^{III}$PP, which have nearly the same C_t–N distances; the former is domed[21] while the latter is flat.[22] The agreement

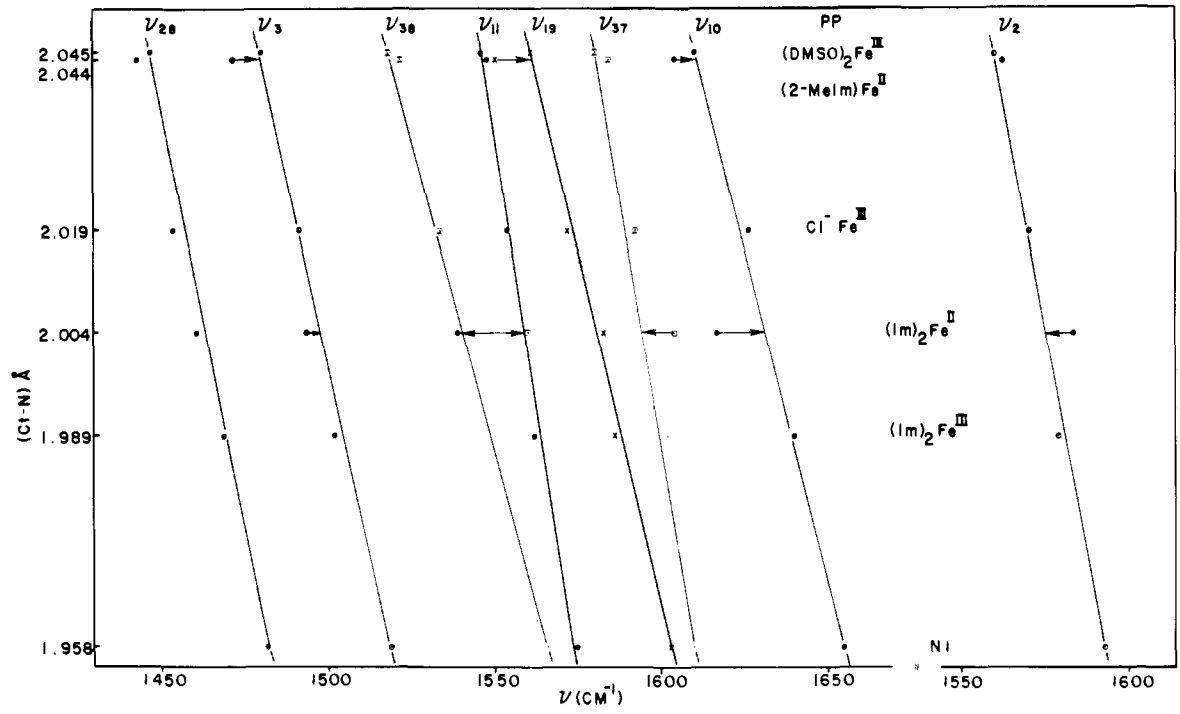

Figure 4. Porphyrin skeletal mode frequencies (above 1450 cm^{-1}) vs. porphyrin core size for the complexes in this study. C_t–N distances used for the PP complexes are as follows: 1.958 Å, NiOEP (D_{4h});[17] 1.989 Å, $[Im_2Fe^{III}TPP]Cl^-$;[18] 2.004 Å, $Im_2Fe^{II}TPP$;[19] 2.019 Å, $ClFe^{III}PP$;[20a*] 2.044 Å, $(2\text{-MeIm})Fe^{II}TPP$;[21] 2.045 Å, $[(Me_2SO)_2Fe^{III}TPP]ClO_4^-$.[22] The symbols indicate the RR polarizations: (●) polarized; (○) depolarized; ×, anomalously polarized; □, E_u. The discrepant points of $Im_2Fe^{II}PP$ and $(2\text{-MeIm})Fe^{II}PP$ are indicated by arrows. (* This is the average C_t–N distance for 5-coordinate high-spin Fe^{III} complexes given by Hoard.[20a] There is actually substantial variation in the C_t–N distance reported for individual structures: 2.027 Å for $(Fe^{III}TPP)_2O$,[20b] 2.022 Å for $(CH_3O)Fe^{III}MP$ (dimethyl ester),[20c] and 2.007 Å for $ClFe^{III}PP$[20d] itself. We find, however, that the skeletal mode frequencies are the same for $(Fe^{III}PP)_2O$ as for $ClFe^{III}PP$, and we surmise that the anomalously low C_t–N distance reported for the latter may be in error or else that it reflects unusual packing forces in the crystal.)

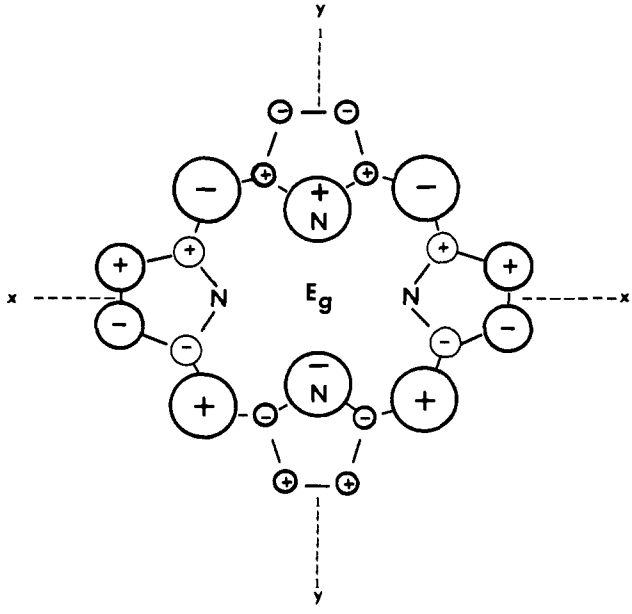

Figure 5. Porphine e_g* orbital[24] (one of the degenerate pair). The signs refer to the p_z atomic orbitals, and the sizes of the circles are proportional to their coefficients.

is generally good, but the $(2\text{-MeIm})Fe^{II}PP$ frequencies are noticeably lower for ν_{10} (6 cm^{-1}), ν_{19} (10 cm^{-1}), and ν_3 (9 cm^{-1}). It has already been noted that this lowering, observed also in deoxyHb, makes it difficult to be exact about the extent of Fe displacement from the heme plane in the COHb picosecond photoproduct.[25] The ν_{10} and ν_{19} frequencies of the latter are the same as those of the in-plane high-spin complex, $(THF)_2Fe^{II}OEP$ (THF = tetrahydrofuran) (ν_{10} = 1605 cm^{-1}, ν_{19} = 1551 cm^{-1}).[25] These frequencies agree with the values calculated from the present correlations for the expanded core (C_t–N = 2.057 Å) of the analogous tetraphenylporphyrin complex.[33] The doming effect, however, reduces the extent of the differences between these frequencies and those of deoxyHb.[25]

(d) Skeletal Modes below 1450 cm^{-1}. The only prominent mode below 1450 cm^{-1} is ν_4 (A_{1g}) which is largely C_aN stretching in character.[2b] Its frequency was noticed to be diagnostic of the Fe oxidation state in early studies.[7,10] Indeed the band is found at 1373 cm^{-1} for both $Im_2Fe^{III}PP^+$ and $ClFe^{III}PP$ and only 3 cm^{-1} lower for $(Me_2SO)_2Fe^{III}PP^+$, despite the large differences in core size of these Fe^{III} complexes. Evidently C_aN stretching is insensitive to core size but depends instead on the polarization of the pyrrole nitrogen by the effective nuclear charge of the central metal; the frequency is 8 cm^{-1} higher for Ni^{II}, whose effective nuclear charge is expected to be greater. The much lower frequency, 1357 cm^{-1}, of $(2\text{-MeIm})Fe^{II}PP$ may be a reflection of the lowered effective nuclear charge for high-spin Fe^{II}, since back-bonding is unimportant and the effect of doming on C_aN stretching is expected to be slight. For $Im_2Fe^{II}PP$, however, the lowered frequency, 1359 cm^{-1}, is attributable to back-bonding (see above) rather than nuclear charge per se. As with ν_{11} and ν_{10}, the frequency is raised when π acid ligands replace imidazole.[9]

For the remaining, skeletal, modes, the frequency variations among the different complexes are small, and in some cases uncertain, due to the difficulty of resolving weak, overlapping bands (e.g., ν_{20} and ν_{29} at ~1400 cm^{-1}). The elevated frequency of the $Im_2Fe^{II}PP$ C_b–vinyl stretch (1174 cm^{-1} vs. 1167–1170 cm^{-1} for all the other complexes) may again be associated with back-bonding.

(e) Peripheral Substituent Effects. The preceding study[3] on NiPP and NiOEP demonstrated that the vinyl groups of PP selectively perturb the frequencies of those skeletal modes that are coupled to the vinyl vibrations. Thus ν_2 (A_{1g}), which primarily involves C_b–C_b stretching, is coupled with vinyl C=C stretching (as shown by a 3-cm^{-1} downshift upon vinyl C_α deuteration[3]) and

(25) Terner, J.; Stong, J. D.; Spiro, T. G.; Nagumo, M.; Nicol, M.; El-Sayed, M. A. *Proc. Natl. Acad. Sci. U.S.A.* **1981**, *78*, 1313.

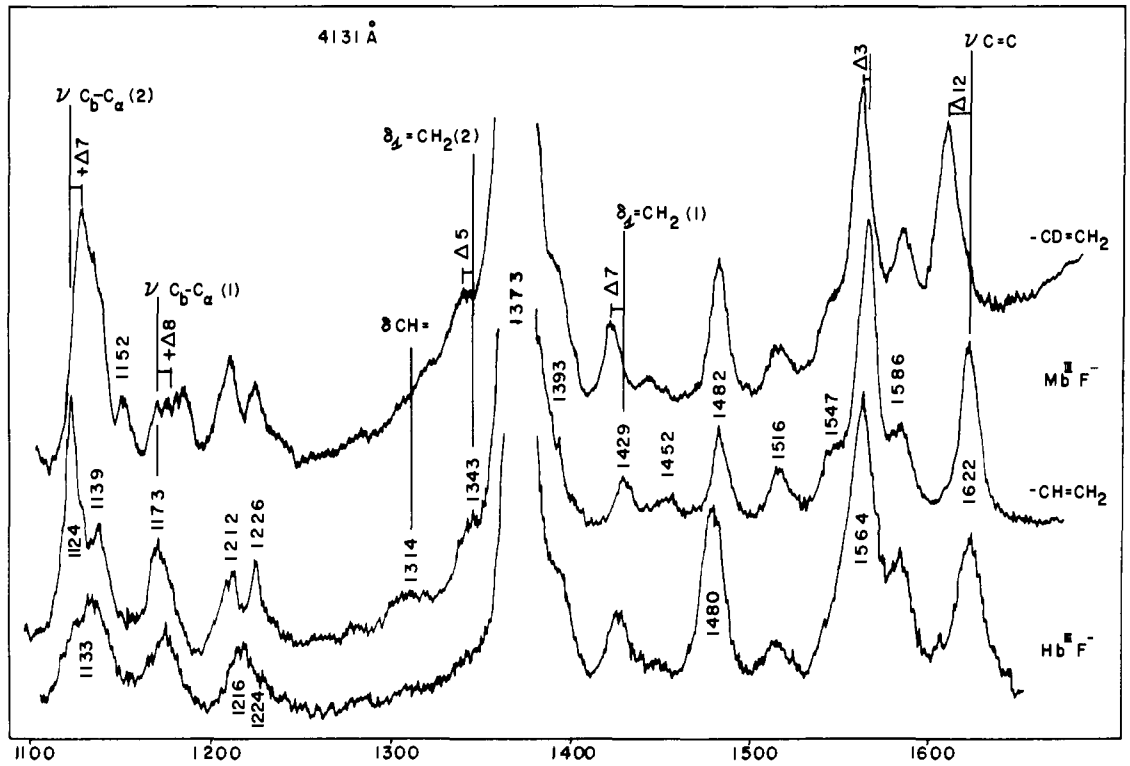

Figure 6. Raman spectra of $Hb^{III}F$, $Mb^{III}F$, and $Mb^{III}F$ reconstituted with $ClFe^{III}PP$-d_α, with 4131-Å Kr^+ excitation (100 mW); heme concentrations, ca. 0.05 mM in phosphate buffer (0.05 M, pH 6.5); slit width, 5 cm^{-1}.

its frequency is 9 cm^{-1} lower in NiPP than in NiOEP. Likewise ν_{29} (B_{2g}) and ν_{20} (A_{2g}) are shifted down by 8 cm^{-1} and up by 3 cm^{-1}, respectively, due to coupling with the vinyl $=CH_2$ scissors modes. The data in Table I show that similar shifts are seen when mesoporphyrin (MP) or OEP complexes of Fe are compared with their PP analogues.

Callahan and Babcock[23] have also noted ν_2 frequency differences between Fe complexes of PP and saturated analogues (OEP and etioporphyrin). Interestingly, they found that heme *a* analogues have ν_2 frequencies lying closer to the saturated porphyrins than to PP, even though heme *a* has a vinyl as well as a formyl substituent. The data of Tsubaki et al.,[26] on myoglobin reconstituted with hemes whose vinyl groups are selectively converted to formyl groups, indicate that the position of the substituent is important. Thus their deoxyMb spectra show a band (ν_2) at 1566 and 1565 cm^{-1} for both 2,4-vinyl (native) and 2-vinyl-4-formyl but at 1555 cm^{-1} for 2-formyl-4-vinyl. Likewise ν_4 is seen at 1357 and 1355 cm^{-1} for the former two species, but at 1350 cm^{-1} for the latter. Formyl substitution has a substantial effect on these skeletal modes when carried out at position 2 but not at position 4. It is not clear whether the effect is due to the different positions per se or to protein influences acting differentially on the substituents, since protein-free spectra were not obtained. The absorption spectra of Sono and Asakura[27] do show absorption spectral differences for these positional isomers in reconstituted myoglobin but not in the protein-free hemes.

When ν_2 is examined for the MP complexes included in this study (Table I), it is seen that the difference with respect to PP grows as the frequency of ν_2 decreases (i.e., as C_t–N increases). The difference is 13 cm^{-1} for Im_2Fe^{III} but 20 cm^{-1} for $(Me_2SO)_2Fe^{III}$. Consequently the ν_2 core-size dependence is less pronounced for MP than for PP. This is a surprising result, since the vinyl ν(C=C) frequency does not decrease in parallel with ν_2 and vibrational coupling between ν(C=C) and ν_2 should decrease with decreasing ν_2. Thus the differential effect must be due to electronic factors, i.e., vinyl conjugation, which can be expected to lower ν_2.

A similar effect is seen for ν_{11} (B_{1g}), which is also mainly C_b–C_b stretching in character. NiPP shows the same ν_{11} frequency as NiOEP, and no C_α deuteration shift is observed, indicating that coupling with ν(C=C) is negligible (due no doubt to the larger frequency separation). For iron complexes, however, a frequency difference of 6–9 cm^{-1} is observed for ν_{11} between PP and MP or OEP. As noted above this band is highly sensitive to π delocalization; it had previously been recognized that its frequency is somewhat different for heme proteins and mesoporphyrin analogues.[28]

Complex vinyl effects are observed in the 950–1300-cm^{-1} region, where major contributions from C_b-substituent stretchings are expected. The 1234-cm^{-1} NiPP band is 14 cm^{-1} higher than the corresponding mode (ν_{13}, B_{1g}) in NiOEP, but for the Fe complexes the changes in this band are much smaller, and variable (−3 to +6 cm^{-1}) between PP and OEP or MP. The 1167-cm^{-1} band (C_b–vinyl stretch, correlating with ν_{30}, B_{2g} of OEP) decreases 7–9 cm^{-1} between PP and OEP or MP for Ni^{II}, Im_2Fe^{III}, and (2-MeIm)Fe^{II}. But for Im_2Fe^{II}, the PP band, which is elevated to 1174 cm^{-1}, appears to split in MP to 1175 and 1154 cm^{-1}. This curious effect is not understood. For the 1130-cm^{-1} band (assigned by Kitagawa et al.[2a] to a combination mode, $\nu_6 + \nu_8$ (A_{1g})), there is a difference between OEP and MP. The PP frequency is 8 and 11 cm^{-1} lower than the OEP frequency for Ni^{II} and Im_2Fe^{III}, but the MP frequency is the same as the PP frequency for Im_2Fe^{III} and Im_2Fe^{II} and 6 cm^{-1} lower for (2-MeIm)Fe^{II} and 3 cm^{-1} higher for $(Me_2SO)_2Fe^{III}$.

For NiPP the 1025-cm^{-1} NiOEP band (ν_5, A_{1g}) is missing, while a new band appears at 999 cm^{-1}. The same switch is observed between $Im_2Fe^{III}PP^+$ and $Im_2Fe^{III}OEP^+$, but $Im_2Fe^{III}MP^+$ has a band at 1001 cm^{-1}, while $Im_2Fe^{II}MP$ has bands at both 1020 and 996 cm^{-1}. We prepared the meso-deuterated derivative, $Im_2Fe^{II}PP$-d_4, and found that the 995-cm^{-1} band shifted down by 23 cm^{-1}, while an IR band of $ClFe^{III}PP$ at 984 cm^{-1} was also downshifted (~16 cm^{-1}). Assignment of these bands to components of the E_u mode ν_{45}, which shifts from 993 to 943 cm^{-1} in NiOEP-d_4,[2] is therefore suggested. The 1025-cm^{-1} (ν_5) NiOEP

(26) Tsubaki, M.; Nagai, K.; Kitagawa, T. *Biochemistry* **1980**, *19*, 379.
(27) Sono, M.; Asakura, T. *J. Biol. Chem.* **1975**, *250*, 5227.
(28) Stong, J. D.; Burke, J. M.; Daly, P.; Wright, P.; Spiro, T. G. *J. Am. Chem. Soc.* **1980**, *102*, 5815.

Table III. Raman Frequencies of Protoheme Proteins and Their Analogues[a]

assignments[a]			$Mb^{III}F$	$Hb^{III}F$	$(Me_2SO)_2Fe^{III}PP$	Mb	(2-MeIm)$Fe^{II}PP$	vinyl modes
ν_{10}	B_{1g}	C_aC_m	1607	1610	1610	1607	1604	
			1622	1622	1621	1618	1622	ν(C=C)
ν_{37}	E_u	C_bC_b	1586	1585	1580	1584	1583	
ν_{19}	A_{2g}	C_aC_m	1557		1560	1552	1550	
ν_2	A_{1g}	C_bC_b	1565	1564	1559	1563	1562	
ν_{11}	B_{1g}	C_bC_b	1547	1550	1545	1546	1547	
ν_{38}	E_u	C_aC_m	1516	1515	1518	1523	1521	
ν_3	A_{1g}	C_aC_m	1482	1480	1480	1473	1471	
ν_{28}	B_{2g}	C_aC_m	1452	1454	1447	1452		
			1429	1427	1429	1426	1426	$\delta_s(=CH_2)$ (1)
ν_{29}	B_{2g}	C_aC_b	1393	1392	1392	1391	1392	
ν_{20}	A_{2g}	C_aN	1391		1389	1395	1401	
ν_4	A_{1g}	C_aN	1373	1372	1370	1357	1357	
			1343	1345		1338	1338	$\delta_s(=CH_2)$ (2)
ν_{21}	A_{2g}	$\delta(C_mH)$	1306	1312	1313	1303	1302	
			1314	1309	1311	1304	1305	δ(CH=)
ν_{13}	B_{1g}	$\delta(C_mH)$	1226	1224	1225		1227	
$\nu_5 + \nu_{18}$	B_{1g}		1212	1216		1213		
ν_{30}	B_{2g}	C_b–S	1173	1173	1170	1173	1170	$\nu(C_b–C_\alpha)$ (1)
$\nu_6 + \nu_8$	A_{1g}		1139	1133	1130	1136	1130	
ν_{44}	E_u	C_b–S	1124		* [b]	1117		$\nu(C_b–C_\alpha)$ (2)
ν_{45}	E_u	C_aN	991	999	*		999	
			1006	1008	*		1005	γ(CH=)

[a] Observed vinyl deuteration downshifts or upshifts (+) (cm^{-1}) are listed here in the order: $Mb^{III}F$-d_α, Mb-d_α: ν(C=C) 12, 12; $\delta_s(=CH_2)$ (1) 7, 4; $\delta_s(=CH_2)$ (2) 5, –; δ(CH=) 223, –; $\nu(C_b–C_\alpha)$ (1) +8, +5; $\nu(C_b–C_\alpha)$ (2) +7, +5. [b] * = obscured by solvent.

band does not shift on deuteration.[2] The RR activation of these two modes is evidently a subtle function of the electronic structure.

The complexities of the 950–1300-cm^{-1} region are worth exploring further, since the bands in this region may prove to be the most sensitive RR monitors of heme–protein interactions (see next section). The spectra reported by Tsubaki et al.[26] also show substantial differences in this region for substituent modification at the two alternative vinyl positions.

Protein Influences. Figure 6 shows RR spectra for the fluoride adducts of metmyoglobin and methemoglobin ($Mb^{III}F$ and $Hb^{III}F$) obtained with 4131-Å excitation, near the maximum of the B band (407 nm). Also shown is the spectrum of $Mb^{III}F$ reconstituted with C_α deuterated protoheme. Table III gives a band-for-band comparison of these proteins with $(Me_2SO)_2Fe^{III}PP^+$, a high-spin six-coordinate analogue,[29] and of deoxyMb with its five-coordinate analogue (2-MeIm)$Fe^{II}PP$.[30] Also listed are the C_α deuteration shifts for $Mb^{III}F$ and deoxyMb.

For deoxyMb the frequencies above 1300 cm^{-1} are all within 3 cm^{-1} of those of (2-MeIm)$Fe^{II}PP$; this includes all the core-size sensitive modes as well as the vinyl C=C stretch and $=CH_2$ scissors modes. Likewise the agreement in this region between $Mb^{III}F$ or $Hb^{III}F$ and $(Me_2SO)_2Fe^{III}PP^+$ is within 3 cm^{-1} for all except two bands. Both ν_2 (A_{1g}) and ν_{37} (E_u), at 1559 and 1580 cm^{-1}, are 6 cm^{-1} lower in the analogue than in the proteins. The nature of the protein influence responsible for these shifts can only be conjectured at this point. ν_2 is the mode that is most strongly coupled with the vinyl C=C stretch. This coupling might be influenced by the orientations of the vinyl groups, which is fixed by the globin contacts in the proteins. However, altered coupling might also be expected to shift the position of ν(C=C) at 1622 cm^{-1}, and this is not observed. Even differences smaller than 3 cm^{-1} can be detected via difference techniques[31] and may be significant in carefully controlled systems. The present comparison reinforces the impression gained from previous work[6] that protein-induced shifts of the heme frequencies above 1300 cm^{-1} are much smaller than those induced by changes in spin and ligation state.

Below 1300 cm^{-1}, protein effects are more dramatic, as might be expected, since the modes involve C_b-substituent stretching directly and should be sensitive to specific globin contacts. The weak ~1260-cm^{-1} band generally observed in the complexes is not seen in the proteins, but a new band is observed at 1212 cm^{-1} (1216 cm^{-1} for $Hb^{III}F$). This may be the $\nu_5 + \nu_{18}$ overtone assigned by Kitagawa et al.[2] at 1220 cm^{-1} in NiOEP. The 1130-cm^{-1} band shifts up significantly in the proteins and by different amounts: 3, 6, and 9 cm^{-1} for $Hb^{III}F$, deoxyMb, and $Mb^{III}F$, respectively.

Most striking is the appearance of a strong new band on the low-energy side of the ~1130-cm^{-1} band in $Mb^{III}F$ (1124 cm^{-1}) and deoxyMb (1117 cm^{-1}) but not in $Hb^{III}F$. This band shifts up, by 5–7 cm^{-1}, upon C_α deuteration, identifying it as a C_b–vinyl stretch.[3] It correlates with the 1113-cm^{-1} E_u mode (ν_{44}) of NiOEP, which appears at 1118 cm^{-1} in the NiPP IR spectrum, shifting up by 12 cm^{-1} on C_α deuteration.[3] This IR band is not activated in the RR spectra of the protein-free complexes, nor apparently in $Hb^{III}F$. (We cannot be sure that it is absent from the 1133-cm^{-1} band envelope of $Hb^{III}F$, since reconstitution with C_α deuterated heme has not been carried out for hemoglobin, but it is certainly less pronounced than in $Mb^{III}F$.) Its strong activation in $Mb^{III}F$ and deoxyMb requires an additional symmetry-lowering effect of the myoglobin pocket; the most effective mechanism would be an electrostatic field, generated by charged groups, or dipoles, localized near the heme vinyl groups. This could induce an excited-state origin shift in an otherwise Raman-inactive mode. Such a field has been calculated for hemoglobin by Warshel,[32] who has suggested that it may modulate O_2 affinity and control cooperativity. The present observations suggest that a similar but larger field may exist in myoglobin.

Acknowledgment. This work was supported by NIH Grants HL 12526 (to T.G.S.), HL 22252 (to K.M.S.) and HL 16087 (to G.N.L.M.).

Registry No. NiPP, 15415-30-2; NiPP dimethyl ester, 15304-70-8; $Im_2Fe^{III}PP^+Cl^-$, 18661-46-6; $Im_2Fe^{III}PP^+Cl^-$ dimethyl ester, 20467-68-9; $Im_2Fe^{II}PP$, 20861-23-8; $ClFe^{III}PP$, 16009-13-5; $(DMSO)_2Fe^{III}PP^+Cl^-$, 82113-38-0; (2-MeIm)$Fe^{II}PP$, 70085-59-5; NiOEP, 24803-99-4; $Im_2Fe^{III}MP^+Cl^-$, 52729-94-9; $Im_2Fe^{III}OEP^+Cl^-$, 41675-39-2; $Im_2Fe^{II}MP$, 20861-21-6; $(DMSO)_2Fe^{III}MP^+Cl^-$, 82113-39-1; (2-MeIm)$Fe^{II}MP$, 82113-40-4; NiPP-d_α, 82113-41-5; NiPP-$d_{2\beta}$, 82113-42-6; $Im_2Fe^{III}PP^+Cl^-$-d_α, 82113-43-7; $Im_2Fe^{III}PP^+Cl^-$-$d_{2\beta}$, 82113-44-8; $Im_2Fe^{II}PP$-d_α, 82135-14-6; $ClFe^{III}PP$-d_α, 82113-45-9; $(DMSO)_2Fe^{III}PP^+Cl^-$-d_α, 82113-46-0; (2-MeIm)$Fe^{II}PP$-d_α, 82113-47-1.

(29) Zobrist, M.; La Mar, G. N. *J. Am. Chem. Soc.* **1978**, *100*, 1944.
(30) Collman, J. P.; Brauman, J. I.; Rose, E.; Suslick, K. S. *J. Am. Chem. Soc.* **1978**, *100*, 6769.
(31) Rousseau, D. L.; Shelnutt, J. A.; Henry, E. R.; Simon, S. R. *Nature (London)* **1980**, *285*, 49.
(32) Warshel, A.; Weiss, R. M. *J. Am. Chem. Soc.* **1981**, *103*, 446.
(33) Reed, C. A.; Mashiko, T.; Scheidt, W. R.; Spartalian, K.; Lang, G. *J. Am. Chem. Soc.* **1980**, *102*, 2302.